

Nadiya Klep

Department of Material Science and Engineering Clemson University, Clemson SC, 29631

(864) 637-9604

nklep@clemson.edu

David Pelot

Department of Mechanical & Industrial Engineering, University of Illinois at Chicago, Chicago,

IL, 60607

(312) 996-3439

dpelot2@uic.edu

Dr. Alexander Yarin

Department of Mechanical & Industrial Engineering, University of Illinois at Chicago, Chicago,

IL, 60607

(312) 996-3472

ayarin@uic.edu

Spreading of a Herschel-Bulkley fluid using lubrication approximation

Abstract:

In this work the flow of 1.5% Carbopol-940 solution was studied as it was transported through a wedge like system at different angles, entrance heights, exit heights, and velocities. The high-speed video of the event was processed by tracking particles entrapped in the solution. This data was used to find the velocity field beneath the wedge. Also, the forces of the fluid (normal and shear) were measured. The known theory of lubrication approximation for Newtonian fluids was used for comparison to the experimental results. It was found that Herschel-Bulkley fluids exhibit similar behavior, such as backflow and stress under the angled plate, to the Newtonian fluid. Furthermore, empirical results for the viscosity of the fluid show a small variance and agree with those found from the viscometer. Overall, this work proves that the lubrication approximation can be used with a highly non-Newtonian fluid and at angles at least up to 20 degrees.

1. Introduction:

The spreading of viscous fluids is something that is encountered in everyday life. From creams, lotions, foods, and construction materials, spreading behavior is one of the main things considered during the preparation process. The motivation behind this study is to model the spreading of soft solid materials, which can be described as Herschel-Bulkley fluid. A Herschel-Bulkley fluid has a shear rate dependent viscosity and a yield stress, meaning that it can be spread onto a surface without running or dripping. Creating a product that can be applied

smoothly and quickly is a competitive advantage for a company which can lead to a more profitable business for both the supplier and buyer.

In order to model such a compound, a well-known transparent Herschel-Bulkley fluid was used. Carbopol-940®, a high molecular weight polyacrylic acid (PAA), is a commercially available thickener often used as an ideal non-Newtonian fluid.¹ According to the manufacturer (Lubrizol®), it has high relative viscosity (similar to joint compound), high shear tolerance (similar to joint compound), and is a clear gel when neutralized.² Carbopol's shear thinning behavior can be described by the Herschel-Bulkley model

$$\tau < \tau_c \Rightarrow \dot{\gamma} = 0; \quad \tau > \tau_c \Rightarrow \tau = \tau_c + K\dot{\gamma}^n \quad (1)$$

where τ and $\dot{\gamma}$ are the shear stress and shear rate, respectively, τ_c is the yield stress of Carbopol and K and n are the consistency index and the behavior index, respectively.³

2. Experimental:

2.1 Fluid preparation

A 1.5% Carbopol-940® (Lubrizol) aqueous solution was prepared by following Novéan's specifications. First, 30 g of Carbopol powder was dissolved in 1970 mL of water. The Carbopol was slowly added to the water, while stirring on a hot plate at 50°C, with a magnetic stirrer set to the highest sustainable setting. The solution was allowed to stir overnight. Next, a NaOH solution was prepared by dissolving 2.8 g of NaOH pellets in 70 mL of water. Finally, the acidic Carbopol solution was neutralized by slowly adding 1 M NaOH and checking the pH with pH-strips. Tracer particles (washed coffee grinds) were mixed in once the Carbopol-940 solution was prepared.

2.2 Rheological measurement

The flow curve of the Carbopol solution was measured using DHR-2 (TA Instruments) shear viscometer. This viscometer measures viscosity using a vane tool. The vane tool had four rectangular blades that protrude from a cylinder to create an outer diameter of 2.80 cm. It was positioned inside a cup that had an inner diameter of 3.02 cm. Each fin of the vane had a height of 4.22 cm, protruded from the inner cylinder by 1.00 cm, and had an outer edge thickness of 0.12 cm which increased to 0.20 cm where it connects to the inner cylinder. The vane tool was calibrated using standard Silicone oil (Brookfield Eng.) with the viscosity of 0.498 Pa s. To calibrate the vane tool the fluid was tested at several shear rates, and then a calibration factor in the software was adjusted accordingly. The shear strain rate was ramped up from 0.1 s^{-1} to 1000 s^{-1} and held constant at each speed for 20 s in all the experiments. The shear rate for the vane tool was calculated as $\dot{\gamma} = \omega(R_0 + R_i)(R_0 - R_i)^{-1} / 2$, where ω is the angular velocity, R_0 is the outer radius, and R_i is the inner radius.

2.3 Apparatus set up

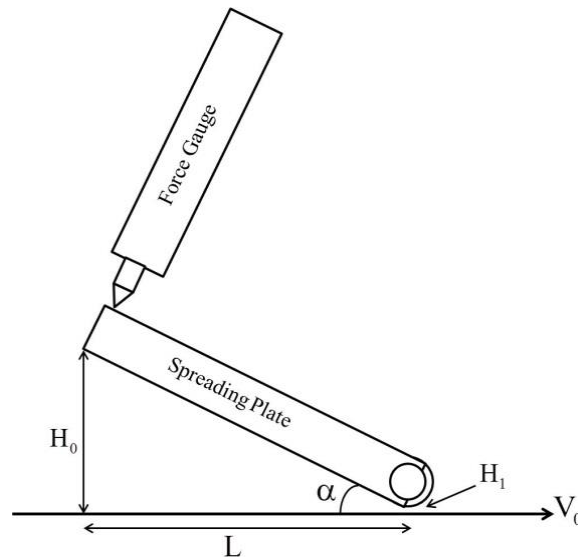


Figure 1. Sketch of experimental setup. Entrance height, H_0 , exit height, H_1 , length, L , angle, α , and velocity of moving bottom plate, V_0 , are labeled.

The wedge-flow meter of length L (**Fig. 1**) consists of a mobile bottom plate with an adjustable velocity (V_0) and a stationary spreading plate, which can be adjusted to the desired angle, α , and an adjustable entrance height, H_0 . A force gauge (IMADA model DS2-11) is fitted normal to the edge of the top plate to measure the force on the fluid as it moves through the system. The set-up was powered by a LEESON A.C. motor (Model: CM38P17EZ12C). The exit height, H_1 , was adjusted to a minimum value between 0.6 mm and 0.8 mm and a maximum value between 1.3 mm and 1.5 mm and the entrance height was adjusted to create angles of 5° , 10° , and 20° . Six experiments were completed combining different H_0 and H_1 values as well as two experiments where the velocity was increased for one angle setting from $0.167 \text{ m}\cdot\text{s}^{-1}$ to $0.24 \text{ m}\cdot\text{s}^{-1}$. A Phantom Miro eX4 high-speed camera (model: MIROEX4-1024MC) was used to record each trial. Then the video data was converted into JPEG images using the Phantom Video Player program.

2.4 Processing techniques

The thickness of the Carbopol gel film was measured with a wet-film thickness gauge after the Carbopol exited the wedge system in order to confirm the exit height of the wedge. The JPEG images were analyzed with the use of a MATLAB R2012a program. The tracer particles were tracked manually to allow for higher accuracy than an automatic tracking program would provide. Then, their velocities were plotted using OriginPro 8.6. Contour graphs were produced for each trial. A dimensionless parameter $\overline{H_0}$ was used to scale the y-axis of the graphs

$$\overline{H_0} = \frac{H_0}{H_1} \quad (2)$$

where H_0 is the entrance height and H_1 is the exit height. Similarly the x-axis was scaled to become a dimensionless \overline{x} scale

$$\bar{x} = \frac{x}{L} \quad (3)$$

where x is the distance from the origin and L is the length created by the projection of the wedge onto the x -axis. Lastly, the force gauge located at $x = 0$ and $y = H_0$ collected data and the maximum value was recorded.

Theoretical discussion

The hydrodynamic theory of lubrication is a well-studied and understood phenomena when it comes to Newtonian fluids under limited conditions. It is applied to journal bearing and extruder screws, where the velocities and pressures are high, the angle between the moving and stationary parts is small, and the viscous forces predominate over inertia forces. Under these conditions the geometry of the system can be reduced to a wedge shape with a moving bottom plate of length, L , and an entrance and exit height, H_0 and H_1 , respectively. Since the velocity in the y -direction, v , is much smaller than the velocity in the x -direction, u , the vertical motion under the wedge is ignored. Using Schlichting's approximations from Boundary Layer Theory ⁴

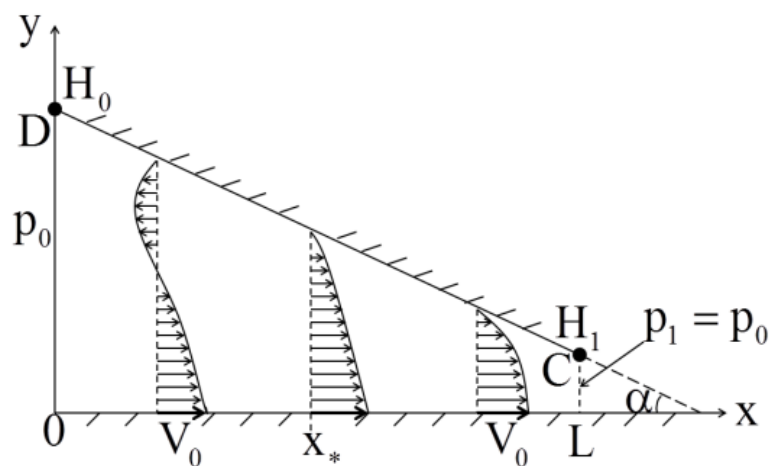


Figure 2. Coordinate axis of the experimental setup with velocity field shown.

$$\frac{dp}{dx} = \mu \frac{\partial^2 u}{\partial x^2} \quad (4)$$

where $\frac{dp}{dx}$ is the pressure gradient, μ is the viscosity, and $\frac{\partial^2 u}{\partial x^2}$ is the second derivative of velocity in the x direction.

Then, applying boundary conditions of the system

$$\begin{aligned} y = 0: u &= V_0 \\ y = H: u &= 0 \end{aligned} \quad (5)$$

where V_0 is the moving plate velocity and H is the equation of the wedge. The equation for velocity becomes

$$u = V_0 \left(1 - \frac{y}{H}\right) - \frac{H^2}{2\mu} \frac{dp}{dx} \frac{y}{H} \left(1 - \frac{y}{H}\right) \quad (6)$$

Due to conservation, the volume flow in every part of the system must be constant

$$Q = \int_0^{H(x)} u \, dy = \text{const.} \quad (7)$$

Evaluating Eq. (7) and solving for the pressure gradient

$$\frac{dp}{dx} = 12\mu \left(\frac{V_0}{2H^2} - \frac{Q}{H^3} \right) \quad (8)$$

Using the boundary conditions of

$$\begin{aligned} x = 0: p &= p_0 \\ x = L: p &= p_0 \end{aligned} \quad (9)$$

gives

$$p(x) = p_0 + 6\mu V_0 \int_0^x \frac{dx}{H^2} - 12\mu Q \int_0^x \frac{dx}{H^3} \quad (10)$$

where L is the length of the wedge in the x direction, p_0 is the pressure outside the wedge, and

$$Q = \frac{1}{2} V_0 \int_0^L \frac{dx}{H^2} \bigg/ \int_0^L \frac{dx}{H^3} \quad (11)$$

The wedge is flat in this case, therefore, the equation of the wedge can be described as

$$H = \frac{H_1 - H_0}{L} x + H_0 \quad (12)$$

Inserting Eq. (12) into Eq. (10), then solving for the pressure distribution

$$p(x) = p_0 + \frac{6\mu V_0 L}{(H_0^2 - H_1^2)} \frac{(H_1 - H)(H - H_2)}{H^2} \quad (13)$$

The force due to the normal stresses can be found as

$$F_{xx} = \int_0^L \sigma_{xx} dx = \int_0^L \sigma_{yy} dx = \int_0^L p dx = \frac{6\mu V_0 L^2 W}{(\overline{H_0} - 1)^2 \overline{H_1^2}} \left[\ln(\overline{H_0}) - \frac{2(\overline{H_0} - 1)}{(\overline{H_0} + 1)} \right] \quad (14)$$

The force due to the shear stress can be found as

$$F_{xy} = \int_0^L \sigma_{xy} dx = \int_0^L \mu \left(\frac{du}{dy} \right) \bigg|_{y=0} = \frac{\mu V_0 L W}{(\overline{H_0} - 1) \overline{H_1}} \left[4 \ln(\overline{H_0}) - \frac{6(\overline{H_0} - 1)}{(\overline{H_0} + 1)} \right] \quad (15)$$

The width, W , was multiplied to Eqs. (14) and (15) because the force is accumulated across the plate in the z direction. It is approximated that the flow is the same at all z coordinates.

The plate is at an angle with respect to the x axis; therefore, in order to find the normal force on the plate the coordinates have to be resolved.

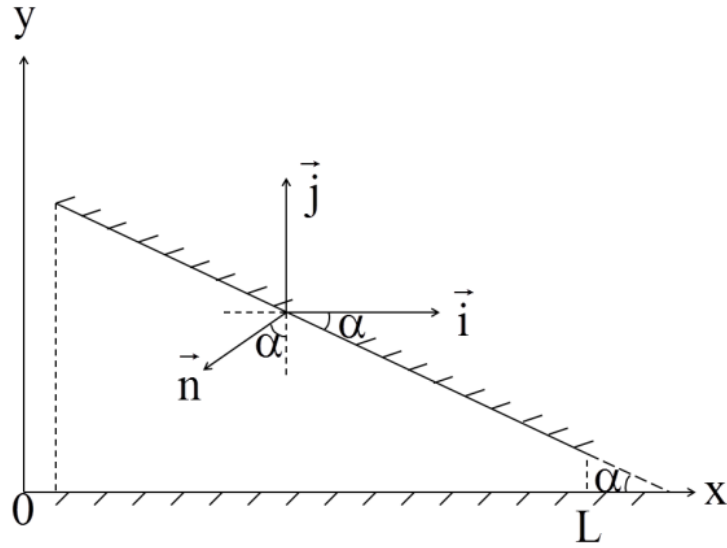


Figure 3. Coordinate sketch showing vector \vec{n} is normal to the top plate.

$$\vec{n} = -\vec{i} \sin(\alpha) - \vec{j} \cos(\alpha) \quad (16)$$

$$\vec{\sigma}_n = \vec{n} \cdot \underline{\underline{\sigma}} \quad (17)$$

$$\sigma_{nn} = \vec{n} \cdot \vec{\sigma}_n = \sin^2(\alpha) \sigma_{xx} + 2\sin(\alpha)\cos(\alpha)\sigma_{xy} + \cos^2(\alpha)\sigma_{yy} \quad (18)$$

$$F_n = \int_0^L \sigma_{nn} \frac{dx}{\cos(\alpha)} \quad (19)$$

Where \vec{n} is the normal vector to the plate, $\vec{\sigma}_n$ is the stress vector normal to the plate, $\underline{\underline{\sigma}}$ is the stress tensor, and F_n is the force normal to the plate. The moment of force balance equation relates the center of pressure, x_c , and the normal force to the position of the force gauge, x_0 , and the experimentally measured force, F_{exp} .

$$F_{exp}(1 - x_0) = F_n(1 - x_c) \quad (20)$$

Where the center of pressure is given by

$$x_c = \frac{1}{2}L \left[\frac{2\overline{H}_0}{\overline{H}_0 - 1} - \frac{\overline{H}_0^2 - 1 - 2\overline{H}_0 \ln(\overline{H}_0)}{(\overline{H}_0^2 - 1) \ln(\overline{H}_0) - 2(\overline{H}_0 - 1)^2} \right] \quad (21)$$

This paper presents data that was collected using a non-Newtonian fluid (Carbopol-940®) flowing through a system with larger angles than those recommended by the current model; however, the theoretical models for force (F) and velocity(**u**) are still of merit, and are used as the control to the experimental results that were collected.

Carbopol-940® is a Herschel-Bulkley fluid, however; after the yield stress, τ_c , is reached it can be modeled by the power-law model

$$\tau = K\dot{\gamma}^n \quad (22)$$

where τ and $\dot{\gamma}$ are the shear stress and shear rate, n is the behavior index, and K is the consistency index. The viscosity can then be expressed as

$$\mu = K\dot{\gamma}^{n-1} \quad (23)$$

The shearing behavior of a power law fluid is represented by a line on a log-log scale. For shear thinning fluids the behavior index, n , is less than one, which correlates to a negative slope on a log-log graph. ⁵

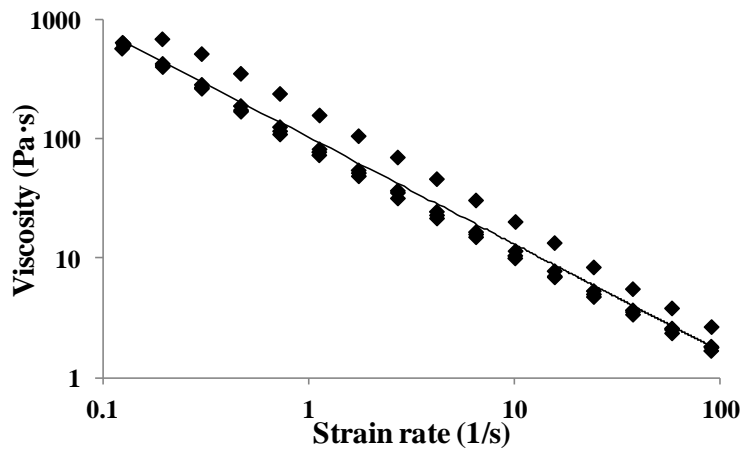
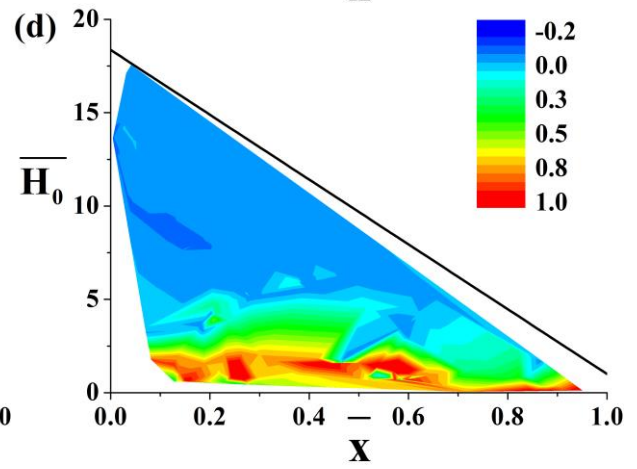
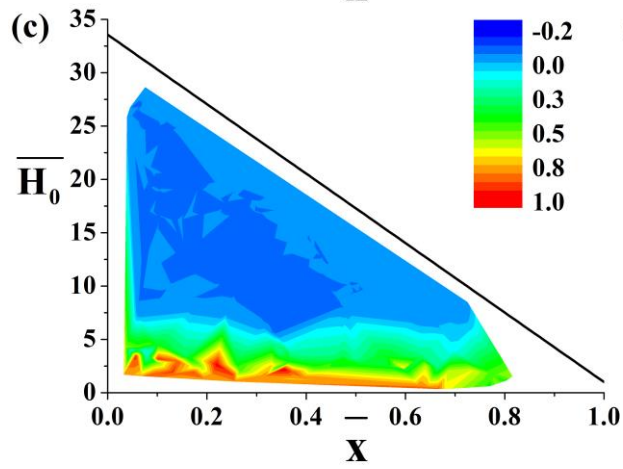
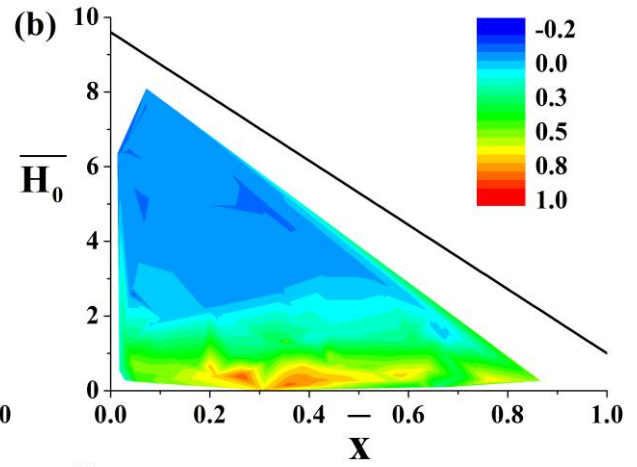
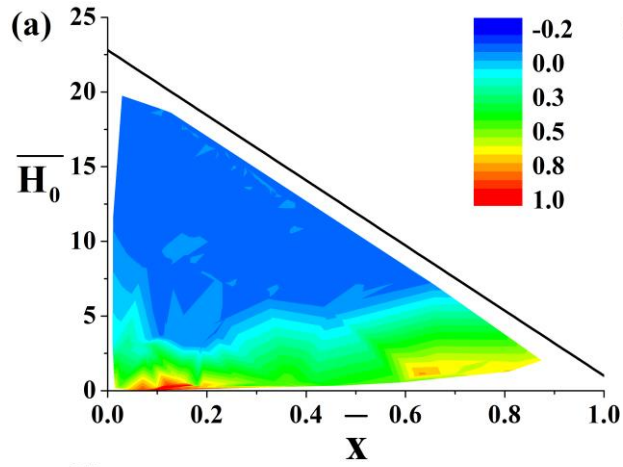


Figure 4. Shows the decrease in the viscosity of the Carbopol from almost 1000 Pa·s at a shear rate of 0.1 s^{-1} to less than 1.5 Pa·s at a shear rate of 90 s^{-1} . The negative slope confirms the shear thinning behavior of Carbopol-940. The fitting line gives values of $n = 0.1$ and $K = 105 \text{ Pa}\cdot\text{s}^n$.

Results and Discussion:

| Trial (Fig. 5) | Angle (deg) | H_1 (mm) | \overline{H}_0 | Velocity ($\text{m}\cdot\text{s}^{-1}$) | Force (N) | Viscosity ($\text{Pa}\cdot\text{s}$) |
|----------------|-------------|------------|------------------|---|-----------|--|
| a | 5 | 0.60 | 23 | 0.167 | 19.1 | 4.7 |
| b | 5 | 1.50 | 10 | 0.167 | 15.0 | 5.9 |
| c | 10 | 0.80 | 34 | 0.167 | 13.5 | 11.4 |
| d | 10 | 1.50 | 18 | 0.167 | 7.9 | 8.3 |
| e | 20 | 0.60 | 87 | 0.167 | 8.1 | 20.2 |
| f | 20 | 1.30 | 40 | 0.167 | 6.8 | 19.5 |
| g | 20 | 0.65 | 80 | 0.240 | 9.8 | 17.2 |
| h | 20 | 1.50 | 35 | 0.240 | 9.7 | 20.0 |

Table 1: Summary of result indicating the name of the trial (a-h) the angle of the wedge, α , the exit height (H_1), the dimensionless scaled entrance height, \overline{H}_0 , velocity of the bottom plate, V_0 , the maximum force measured (F) and the empirically found viscosity, μ .



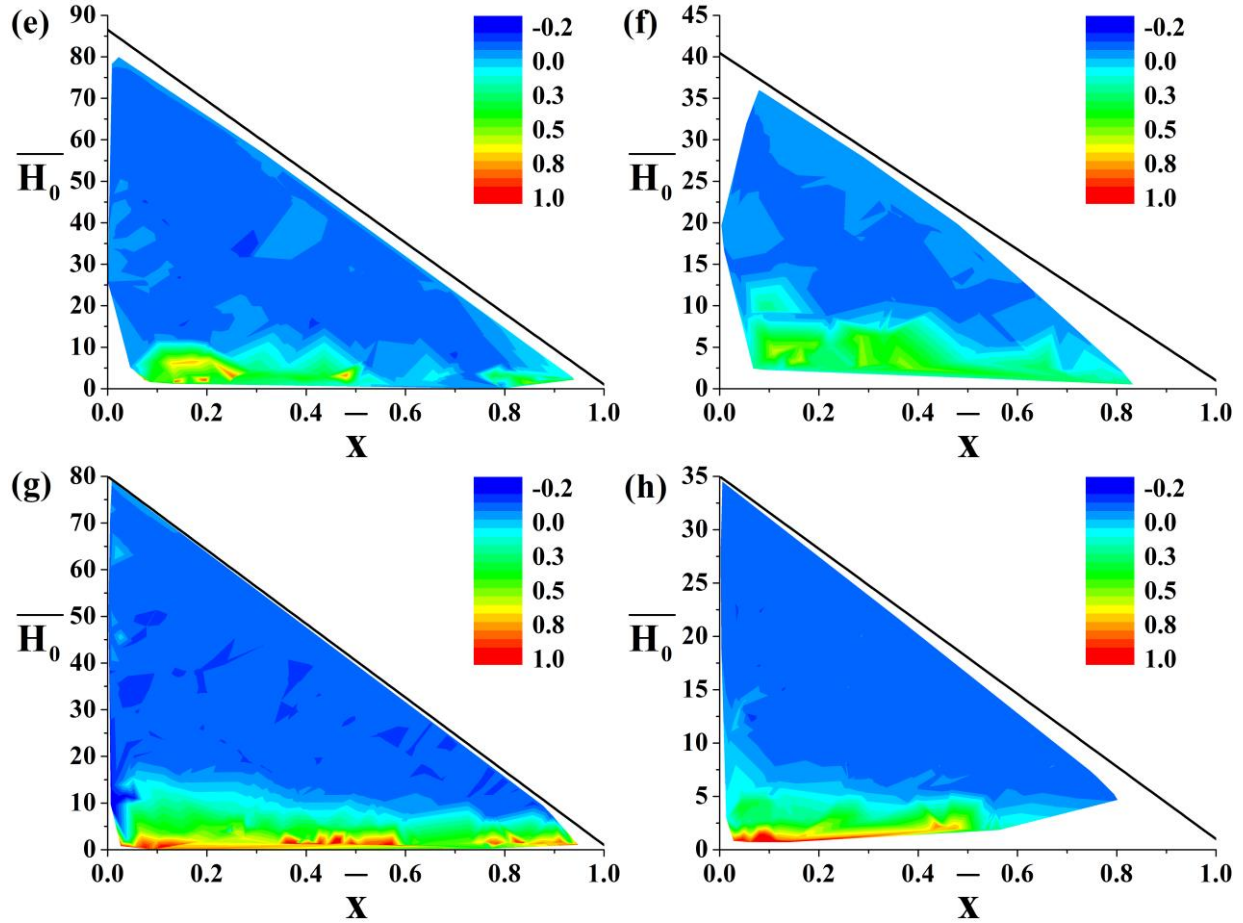


Figure 5. Contour plots showing velocity field for each experiment in Table 1. The legend shows the ratio of velocity to maximum velocity.

As expected from the velocity profile in Eq. 6 (and maybe shown in FIG 2 in beginning of theory), the fluid near the moving plate up to the height of the exit moves at speeds near the maximum velocity, this is shown by colors yellow, orange, and red in Fig.5 When the fluid nears the wedge the movement of the bottom plate is not felt as strongly as the pressure gradient pushing the fluid backwards causing a negative velocity, shown by different shades of blue. In **Figure 5**, the trend of increased and faster backflow can be seen as $\overline{H_0}$ get larger. From graphs **d**: $\overline{H_0}=18$, **c**: $\overline{H_0}=34$, **f**: $\overline{H_0}=40$, to **e**: $\overline{H_0}=87$ the concentration and the intensity (shade) of blue gets

larger indicating a larger amount and faster reverse flow. The graphs are all scaled from -0.2 (dark blue) where the negative indicates reverse flow at 20% of V_0 to 1 (red) which correlates to 100% or V_0 in the forward direction.

The force gauge data in **Table 1** reveals three trends of the fluid that agree with the theory. Keeping the exit height (H_1) constant, the force decreases as $\overline{H_0}$ increases. **Figure 5 a,c,e** $\overline{H_0} = 23, \overline{H_0} = 34, \overline{H_0} = 87$, respectively all have H_1 equal to 0.6 mm to 0.8 mm (the low value) and the forces respectively decrease from 19.1 N, 13.5 N, to 8.05 N. Similarly in the case of H_1 equal to 1.3 mm to 1.5 mm (the high value), **Fig. 5 b,d,f** $\overline{H_0} = 10, \overline{H_0} = 18, \overline{H_0} = 40$, respectively decrease in force from 15.0 N to 7.9 N to 6.8 N. The trend for keeping, $\overline{H_0}$ constant but increasing H_1 , as in trials **a** and **d**, which had $\overline{H_0}$ set at 23 and 15, two relatively close values, the force decreases from 19.1 N to 7.9 N. The same trend was present in trials **c** and **f**, where $\overline{H_0}$ was set to 34 and 40. The force decreased from 13.5 N to 6.8 N as H_1 increased from 0.8 mm to 1.3 mm. The third trend observed was the increase in velocity while keeping both H_1 and $\overline{H_0}$ constant causing the force to increase. From trials **e** and **g**, where H_1 was set between 0.6 mm to 0.65 mm and $\overline{H_0}$ was between 80-87, when the velocity was increased from $0.167 \text{ m}\cdot\text{s}^{-1}$ (**e**) to $0.24 \text{ m}\cdot\text{s}^{-1}$ (**g**) the force increased from 8.05 N to 9.77 N. Also from the contour **g** and **e** (**Fig. 5**) it can be seen that the reverse flow velocity also increases as V_0 increases due to the increase in the intensity of the blue shade from **e** and **g**. The same trend for both reverse flow and increased force were seen in trials **f** and **h** where H_1 was set between 1.3 mm to 1.5 mm and $\overline{H_0}$ was between 35 and 40, when the velocity was increased from $0.167 \text{ m}\cdot\text{s}^{-1}$ (**f**) to $0.24 \text{ m}\cdot\text{s}^{-1}$ (**h**) the force increased from 6.8 N to 9.73 N, and the contour map (**Fig. 5**) from **f** to **h** show increased intensity of blue. The forces due to the normal and shear stress are both proportional to velocity

as in Eqs. (14) and (15); therefore, any increase in velocity should be reflected in a directly proportional increase in force measured. Indeed, the velocity ratio is equal to the force ratio between (f) and (h) and is approximately equal to the force ratio (e) and (g).

The viscosity values shown in **Table 1** were found empirically by equating the theoretical force to the experimental force. Since Carbopol is a shear thinning fluid the viscosity is dependent on shear rate. The maximum shear rate occurs at the exit of the wedge and was found to be approximately 300 s^{-1} and the minimum shear rate occurs at the entrance of the wedge and was found to be approximately 3 s^{-1} . According to **Fig 4** these shear rates correspond to a viscosity of $0.6 \text{ Pa} \cdot \text{s}$ and $39 \text{ Pa} \cdot \text{s}$, respectively. The viscosity values found empirically in **Table 1** are within this viscosity range. Therefore, using a Herschel-Bulkley fluid to model a Newtonian based fluid theory was found to be successful.

Acknowledgments:

The authors would like to thank the National Science Foundation for providing the funding and support for this research project through NSF Grant # 1062943. As well as the program coordinators, Professor Christos Takoudis and Professor Gregory Jursich, for running and organizing this Research Experience for Undergraduates program.

References:

1. Weber, E., Moyers-Gonzalez, M., and Burghelca, T.I., (2012). Thermorheological properties of a Carbopol gel under shear. *Journal of Non-Newtonian Fluid Mechanics*, 183-184(0), 14-24.
2. The Lubrizol Corporation, Technical Data Sheet (TDS-237), Sept. 16, 2009.

3. Coussot, P., Tocquer, L., Lanos C., and Ovarlez G., (2009). Macroscopic vs. local rheology of yield stress fluids. *Journal of Non-Newtonian Fluid Mechanics*, 158(1), 85-90. ISSN 0377-0257
4. Schlichting, H., "Boundary-Layer Theory", 7th edn. McGraw-Hill, Inc. New York, 1987, (116-123).
5. Bonacucina, G., Martelli, S., and Palmieri, G., (2004) Rheological, mucoadhesive and release properties of Carbopol gels in hydrophilic cosolvents, *International Journal of Pharmaceutics*, 282(1), 115-130.